Effect of Disorder on Transport in Graphene

I. L. Aleiner[1] and K. B. Efetov[1,2,3]

[1]*Physics Department, Columbia University, New York, New York 10027, USA*
[2]*Theoretische Physik III, Ruhr-Universität Bochum, 44780 Bochum, Germany*
[3]*L. D. Landau Institute for Theoretical Physics, 117940 Moscow, Russia*

(Received 7 July 2006; published 4 December 2006)

Quenched disorder in graphene is characterized by 5 constants and experiences the logarithmic renormalization even from the spatial scales smaller than the Fermi wavelength. We derive and solve renormalization group equations (RGEs) describing the system at such scales. At larger scales, we derive a nonlinear supermatrix σ model completely describing localization and crossovers between different ensembles. The parameters of this σ model are determined by the solutions of the RGEs.

DOI: 10.1103/PhysRevLett.97.236801 PACS numbers: 73.63.−b, 72.15.Rn, 81.05.Uw

Introduction.—The Dirac spectrum of the quasiparticles in graphene confirmed by recent experiments [1–3] is a consequence of the honeycomb lattice symmetry [4]. Although many properties of graphene can be understood in terms of ballistic motion of "relativistic" electrons described by a Dirac-like equation (see, e.g., [5]), disorder plays an important role in sufficiently large samples.

Influence of disorder on two-dimensional electron gases on the honeycomb lattice was studied in several works [6–12] within a self-consistent Born approximation (SCBA) standard for weakly disordered metals and superconductors. Within SCBA, such quantities as density of states or localizationless conductivity [7–10] were calculated. The weak localization (WL) correction was discussed in Ref. [11] and calculated in Ref. [12]. However, the SCBA is not justifiable for the Dirac spectrum, $|\varepsilon| = v|p|$, as it can be seen already in the fourth order perturbation theory in the disorder potential (see below), and a more careful analysis is needed.

In this Letter, we reveal the origin of the logarithmic effects specific for the Dirac spectrum and different from WL. These corrections (see Fig. 1) are contributed by all spatial scales between the lattice constant a and either wavelength $\lambda_\varepsilon = \hbar v/\varepsilon$ or the scale determined by disorder, and that is why we will coin the name "ultraviolet logarithmic corrections" (uvLC) for them. We will sum up the leading series of uvLC within a one-loop renormalization group (RG). At larger linear scales physics is described by a nonlinear σ model [13] and uvLC enter as renormalized parameters in this model. We will show that the low-energy asymptotics correspond to the orthogonal ensemble. Thus, the one-particle states are localized at any energies in contradiction with the findings of Ref. [1] of the minimal metallic conductivity in the undoped graphene.

Disordered Hamiltonian.—In the undoped graphene two bands cross the Fermi level at K and K' points. The corresponding Bloch functions comprise the basis of the four-dimensional (4D) representation of the planar group of the honeycomb lattice. We join them in a vector

$$\vec{\varphi}^{\,T}(\mathbf{r}) = ((\varphi_A, \varphi_B)_{AB}; (\varphi_B^*, -\varphi_A^*)_{AB})_{KK'}, \qquad (1)$$

where we use the fact the points K and K' are connected to each other by the time-reversal symmetry

$$\vec{\varphi}^{\,*}(\mathbf{r}) = \hat{z}\,\vec{\varphi}(\mathbf{r}), \qquad \hat{z} \equiv \tau_y^{AB} \otimes \tau_y^{KK'}, \qquad (2)$$

where the 4D space of the wave functions is represented as a direct product $AB \otimes KK'$ of the sublattice AB and "valley" KK' 2D spaces, and $\tau^\alpha_{x,y,z}$, $\tau^\alpha_\pm = (\tau_x \pm i\tau_y)/2$ are the Pauli matrices acting in those spaces, $\alpha = AB, KK'$ (we omit the physical spin).

The low-energy properties are described in $k \cdot \mathbf{p}$ approximation [4]; i.e., the wave function $\Psi_\varepsilon(\mathbf{r})$ is looked for as $\Psi_\varepsilon(\mathbf{r}) = \vec{\varphi}(\mathbf{r}) \cdot \vec{\Phi}_\varepsilon(\mathbf{r})$ with a smooth envelope, $\vec{\Phi}_\varepsilon(\mathbf{r})$, satisfying the effective Schrödinger equation ($\hbar = 1$)

$$[\hat{H}_0 + \hat{V}(\mathbf{r})]\vec{\Phi}_\varepsilon(\mathbf{r}) = \varepsilon\vec{\Phi}_\varepsilon(\mathbf{r}), \qquad \hat{H}_0 = -iv\hat{\vec{\Sigma}}\vec{\nabla}, \qquad (3)$$

where $\vec{\nabla} = (\partial_x, \partial_y)$ and we introduced 4×4 matrices [14]

$$\hat{\Sigma}_{x,y} = \mathbb{1}^{KK'} \otimes \tau_{x,y}^{AB}, \qquad \hat{G}_{m,i} = \tau_m^{KK'} \otimes \tau_i^{AB}. \qquad (4)$$

For the spinless particles, the time-reversal symmetry (TRS) requires $\Psi^*(\mathbf{r}) = \vec{\varphi}^*(\mathbf{r}) \cdot \vec{\Phi}^*(\mathbf{r})$ also to be the eigenstate of the original Hamiltonian. Together with Eq. (2) it constrains the effective Hamiltonian from Eq. (3) as

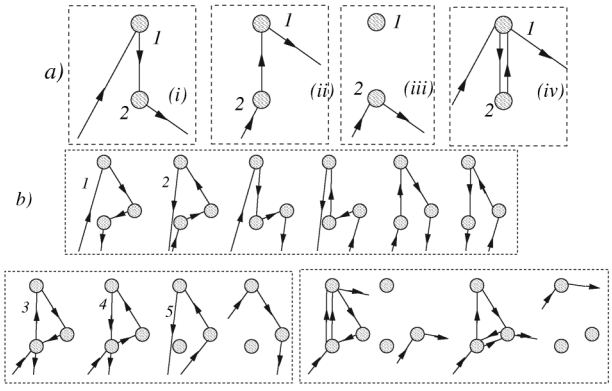

FIG. 1. Interfering scattering events involving (a) two- and (b) three-impurity scattering.

$$\hat{H}_0 = \hat{z}\hat{H}_0^T\hat{z}, \qquad \hat{V} = \hat{z}\hat{V}^T\hat{z}. \tag{5}$$

The disorder, $V(\mathbf{r}) = V^\dagger(\mathbf{r})$, in Eq. (3) may break all the symmetries except that of the TRS (5). This leads to

$$\hat{V}(\mathbf{r}) = \mathbb{1}u_0(\mathbf{r}) + \hat{G}_{m,i}u_{m,i}(\mathbf{r}), \tag{6}$$

where u_0, $u_{m,i}$ are real random functions, $\mathbb{1} \equiv \mathbb{1}^{AB} \otimes \mathbb{1}^{KK'}$, and the summation over indices $\{i, m\} = \{x, y, z\}$ is implied in Eqs. (6) and (7a). Equation (6) is the most general form for the disorder *before* averaging. Averaging must restore the rotational ($\mathcal{D}_6$) and translational symmetries, which leads [15] to the Gaussian correlations

$$\langle \hat{V}_{\mathbf{r}} \otimes \hat{V}'_{\mathbf{r}'} \rangle = \delta_{\mathbf{r},\mathbf{r}'}[\gamma_0 \mathbb{1} \otimes \mathbb{1} + \Gamma^i_m \hat{G}_{m,i} \otimes \hat{G}_{m,i}]. \tag{7a}$$

Coefficients $\Gamma^i_m > 0$ are independent from $\gamma_0 > 0$ and

$$\Gamma^z_z = \gamma_z, \qquad \Gamma^{\{x,y\}}_z = \gamma_\perp, \qquad \Gamma^z_{\{x,y\}} = \beta_z, \qquad \Gamma^{\{x,y\}}_{\{x,y\}} = \beta_\perp, \tag{7b}$$

so that the disorder is characterized by 5 parameters.

Thereinafter, we will treat these parameters γ, β of Eqs. (7) as the starting point of the theory, not calculating their particular values determined by the details of the single impurity on the scale of the lattice constant. However, some conclusions can be drawn from the symmetry arguments [15]. The remote charge impurity potential weakly varying on the scale of the lattice constant a, is invariant with respect to the continuous rotations and generate only the diagonal term ($\gamma_0 > 0, \Gamma^i_m = 0$). A defect in the crystal still preserving the point symmetry $\mathcal{D}_6$ (interstitial atom) generates $\gamma_0 \simeq \beta_z > 0$. A vacancy in a perfect honeycomb lattice preserves $\mathcal{D}_3$ symmetry and allows for $\gamma_z \simeq \gamma_\perp \simeq \beta_\perp \simeq \gamma_0$. Bond disorder ($\mathcal{D}_2$) generates $\gamma_\perp \simeq \beta_\perp \simeq \beta_z \simeq \gamma_0$.

The uvLC originate from the interference of the waves multiply scattered by the disorder potential; however, the configurations of the impurities giving rise to the effect differ from the familiar WL[13]. Thus, it is instructive to explain them first in terms of the counting of the scattering events and then present the rigorous calculation. It will also illuminate reasons for the failure of SCBA.

If there were no disorder potential, the wave function $\vec{\Phi}^{(0)}_{\mathbf{k}}$ would be the plane wave with a momentum $\mathbf{k}$ and the structure of Eq. (1). We limit ourselves by positive energies $\varepsilon = vk$, $k \equiv |\mathbf{k}|$ for concreteness, and the projection operator $\hat{\mathbb{P}}(\mathbf{n}) \equiv (1 + \boldsymbol{\Sigma}\mathbf{n})/2$; $\mathbf{n} = \mathbf{k}/|k|$ chooses the chirality corresponding to the positive energy. Consider an impurity placed at point $\mathbf{R}_1$. The asymptotics of wave function acquire the form $\vec{\Phi}_{\mathbf{k}} = \vec{\Phi}^{(0)}_{\mathbf{k}} + \vec{\Phi}^{(1)}_{\mathbf{k}}$, where

$$\vec{\Phi}^{(1)}_{\mathbf{k}} = \begin{cases} \frac{\exp(\frac{i|\mathbf{r}_1|}{\lambda_\varepsilon})}{\sqrt{-i|\mathbf{r}_1|}} \frac{\hat{\mathbb{P}}(\frac{\mathbf{r}_1}{|\mathbf{r}_1|})\hat{f}_1}{\sqrt{2\pi\lambda_\varepsilon}} \vec{\Phi}^{(0)}_{\mathbf{k}}(\mathbf{R}_1), & \frac{|r_1|}{\lambda_\varepsilon} \gg 1, \\ i(2\pi|\mathbf{r}_1|^2)^{-1}\hat{\boldsymbol{\Sigma}}\mathbf{r}_1\hat{f}_1\vec{\Phi}^{(0)}_{\mathbf{k}}(\mathbf{R}_1), & |r_1| \ll \lambda_\varepsilon, \end{cases} \tag{8}$$

and $\mathbf{r}_1 \equiv \mathbf{r} - \mathbf{R}_1$ is the distance from the impurity.

Equation (8) is valid for both $|\mathbf{r}_1|$ and λ_ε much larger than the characteristic size of the scatterer. All the details of the impurity are encoded in the matrix $\hat{f}_1$ which can be viewed as the scattering length, $a_0 = ||\hat{f}_1\hat{f}_1^\dagger||^{1/2}$. The value of a_0 is of the order of the size of the impurity.

The asymptotic behavior of Eq. (8) at $|r_1| \gg \lambda_\varepsilon$ is nothing but the outgoing spherical wave, corresponding to the s scattering. It is important to emphasize that the dominance of the s channel is the consequence of the large wavelength and not of the peculiarities of the impurity potential. The proportionality coefficient between the spherical wave and the amplitude of the plane wave is the scattering amplitude that enables us to find the elastic scattering cross section of the electron with the original momentum direction $\mathbf{n}_i$ to the final direction $\mathbf{n}_f$:

$$d\hat{s} = \frac{d\mathbf{n}_f}{2\pi\lambda_\varepsilon}[\hat{\mathbb{P}}(\mathbf{n}_f)\hat{f}_1\hat{\mathbb{P}}(\mathbf{n}_i)] \otimes [\hat{\mathbb{P}}(\mathbf{n}_f)\hat{f}_1\hat{\mathbb{P}}(\mathbf{n}_i)]^\dagger. \tag{9}$$

If there were no interference, Eq. (9) would describe all the kinetics of the system. For the impurity density, $n_{\text{imp}} \ll 1/a_0^2$, the mean free path is estimated from

$$\ell_{\text{el}} \simeq (n_{\text{imp}} \parallel \hat{s} \parallel)^{-1} \simeq \lambda_\varepsilon/(n_{\text{imp}}a_0^2) \gg \lambda_\varepsilon. \tag{10}$$

To understand the role of the multiple scattering, consider the two-impurity scattering [see Fig. 1(a), panels (i) and (ii)].

Applying Eq. (8) twice we obtain for $|\mathbf{R}_{12}| \ll \lambda_\varepsilon \ll |\mathbf{r}_1|$, the outgoing wave with $\hat{f}_1 \to \delta\hat{f} = \hat{f}_{12} + \hat{f}_{21}$ and

$$\hat{f}_{(ij)} = -\hat{f}_i\hat{\boldsymbol{\Sigma}}\mathbf{R}_{ij}\hat{f}_j(2\pi|\mathbf{R}_{ij}|^2)^{-1}, \qquad \mathbf{R}_{ij} = \mathbf{R}_i - \mathbf{R}_j, \tag{11}$$

for $i, j = 1, 2$, $i \neq j$, and $a_0 \lesssim |\mathbf{R}_{12}| \lesssim \lambda_\varepsilon$. Equation (11) describes the two-impurity scattering amplitude for the given configuration of the impurities. The transport [see Eqs. (9) and (10)] is determined by the powers of the $\hat{f}_{(ij)}$ averaged with respect to all configurations:

$$\begin{aligned}\langle \hat{f}_{(ij)} \otimes \hat{f}^\dagger_{(ij)} \rangle &= n_{\text{imp}} \int \frac{d^2\mathbf{R}}{4\pi^2R^4}[\hat{f}_i\hat{\boldsymbol{\Sigma}}\mathbf{R}\hat{f}_j] \otimes [\hat{f}_j^\dagger\hat{\boldsymbol{\Sigma}}\mathbf{R}\hat{f}_i^\dagger] \\ &\simeq (4\pi)^{-1}n_{\text{imp}}\mathcal{L}[\hat{f}_i\hat{\Sigma}_\alpha\hat{f}_j] \otimes [\hat{f}_j^\dagger\hat{\Sigma}_\alpha\hat{f}_i^\dagger],\end{aligned} \tag{12a}$$

where $\mathcal{L} = \ln(\lambda_\varepsilon/a)$. Analogously, we find

$$4\pi\langle \hat{f}_{(ij)} \otimes \hat{f}^\dagger_{(ji)} \rangle \simeq -n_{\text{imp}}\mathcal{L}[\hat{f}_i\hat{\Sigma}_\alpha\hat{f}_j] \otimes [\hat{f}_i^\dagger\hat{\Sigma}_\alpha\hat{f}_j^\dagger]. \tag{12b}$$

Combining Eqs. (12a) and (12b), we obtain

$$4\pi\langle \delta\hat{f} \otimes \delta\hat{f}^\dagger \rangle \simeq n_{\text{imp}}\mathcal{L}d_{ij}^{i'j'}[\hat{f}_i\hat{\Sigma}_\alpha\hat{f}_j] \otimes [\hat{f}_{j'}^\dagger\hat{\Sigma}_\alpha\hat{f}_{i'}^\dagger], \tag{12c}$$

where nonvanishing coefficients are $d_{12}^{12} = d_{21}^{21} = 1$, $d_{12}^{21} = d_{21}^{12} = -1$, and summation over all repeating indices here as well as over $\alpha = x, y$ in Eqs. (12) and (14) is implied.

Equation (12c) is the main result of the qualitative consideration revealing the origin of the logarithmic divergence. The Boltzmann equation neglects those contribu-

tions. SCBA accounts only for the diagonal components d_{12}^{12}, d_{21}^{21} and misses all the other. For the scalar disorder, e.g., it leads to the violating the TRS of the problem.

There are two more sources for the $n_{\rm imp}a^2\mathcal{L}$ corrections. One of them is the correlation of the one-impurity scattering with the two-impurity scattering in which one of the impurities is visited twice as shown in Fig. 1(a), panels (iii) and (iv). The corresponding result is easily obtained from the three-impurity scattering amplitude [cf. Eq. (11)]

$$\hat{f}_{(ijk)} = (\hat{f}_i\hat{\mathbf{\Sigma}}\mathbf{R}_{ij}\hat{f}_j\hat{\mathbf{\Sigma}}\mathbf{R}_{jk}\hat{f}_k)/(4\pi^2|\mathbf{R}_{ij}|^2|\mathbf{R}_{jk}|^2), \quad (13)$$

and we find

$$4\pi\langle\hat{f}_{(121)}\hat{f}_2^\dagger\rangle \simeq n_{\rm imp}\mathcal{L}[\hat{f}_1\hat{\Sigma}_\alpha\hat{f}_2\hat{\Sigma}_\alpha\hat{f}_1]\otimes\hat{f}_2^\dagger. \quad (14)$$

This correction is missing in SCBA. The last logarithmic effect arising in this order is the logarithmic dependence $\propto n_{\rm imp}a^2\varepsilon\ln\varepsilon$ of the averaged forward scattering amplitude. It does not affect scattering processes directly but renormalizes the spectrum of the free Hamiltonian H_0. If one considers the three-impurity configurations [see Fig. 1(b)], starting from Eq. (13), he finds 54 contributions $\propto n_{\rm imp}^2\mathcal{L}^2$, only 6 of which are included in the SCBA.

Interference of few processes is somewhat special as it does not vanish completely even if the distance between impurities is larger than λ_ε. In fact, interferences 1–2 and 3–5 are the first contributions giving rise to the WL correction which is also logarithmic. The WL, however, originates from the spatial scales larger than ℓ_{el}, and that is why they can be separated from the uvLC.

Field theory and RG.—Let us turn to the rigorous calculations using the supersymmetry method. Because of the 4×4 matrix structure of the Hamiltonian [Eqs. (3) and (6)], the supervectors ψ should have 4 times more components than usually used [13], i.e., we need 32 components for calculation of the conductivity. The resulting 32D space can be presented as a direct product of five 2D ones, $AB\otimes KK'\otimes AR\otimes eh\otimes g$, where AR, eh, and g are the retarded-advanced, particle-hole, and the fermion-boson sectors. Averaging over $\hat{V}$ and using Eq. (7a), we find

$$\langle\cdots\rangle = \int\cdots\exp(-L[\psi])\mathcal{D}\psi, \qquad \psi^\dagger\hat{\mathbf{\Lambda}} = \bar{\psi} = [\hat{\mathbb{C}}\psi]^T,$$
$$\hat{\Lambda} = \hat{\Lambda}\otimes\mathbb{1}^{AB}, \qquad \hat{\Lambda} = \tau_z^{AR}\otimes\mathbb{1}^{KK'}\otimes\mathbb{1}^{eh}\otimes\mathbb{1}^{g},$$
$$\hat{\mathbb{C}} = i\hat{C}\otimes\tau_y^{AB} = \hat{z}\otimes\tau_z^{AR}\otimes(\tau_-^{eh}\otimes\mathbb{1}^g - \tau_+^{eh}\otimes\tau_z^g), \quad (15)$$

where $\langle\cdots\rangle$ on the left-hand side stands for any combination of advanced or retarded Green functions $\hat{G}^{A,R} = (\varepsilon\mp\omega/2-\hat{H}_0-\hat{V}\mp i0)^{-1}$ and $\cdots$ on the right-hand side stands for the corresponding sources [13]. The Lagrangian $L[\psi] = L_0[\psi] + L_{\rm int}[\psi]$ is (sum over i, $m = x, y, z$ is implied)

$$L_0[\psi] = i\int\bar{\psi}\left[\varepsilon - \hat{\mathbb{H}}_0 - \hat{\mathbf{\Lambda}}\left(\frac{\omega}{2}+i0\right)\right]\psi d\mathbf{r},$$
$$L_{\rm int}[\psi] = \frac{1}{2}\int[\gamma_0(\bar{\psi}\psi)^2 + \Gamma_m^i(\bar{\psi}\hat{\mathbb{G}}_{m,i}\psi)^2]d\mathbf{r}, \quad (16)$$

where $(\hat{\mathbb{H}}_0, \hat{\mathbb{G}}_{m,i}) = (\hat{H}_0, \hat{G}_{m,i})\otimes\mathbb{1}^g\otimes\mathbb{1}^{AR}\otimes\mathbb{1}^{eh}$.

The perturbation theory in $L_{\rm int}[\psi]$ leads to uvLC, and we can calculate the integral (15) using an RG [16]. We decompose ψ as $\psi = \psi_0 + \tilde{\psi}$, where $\tilde{\psi}$ is slow and ψ_0 is fast, and integrate out ψ_0. We rescale $\tilde{\psi}$ and the coordinates to keep the coefficient in front of ε and the ultraviolet cutoff intact. It gives back Eq. (16), with renormalized couplings γ_0, Γ_m^i [Eq. (7b)] and the velocity v [Eq. (3)]. This yields renormalization group equations (see Ref. [15] for details), which we display for the most interesting case $\gamma_0 \gtrsim \Gamma_m^i$:

$$\begin{aligned}
2\pi v\partial_t v &= -(\gamma_0 + g_\parallel + 2g_\perp);\\
9\pi v^2\partial_t\gamma_0 &\approx 2(g_\parallel^2 + 2g_\perp^2);\\
\pi v^2\partial_t\delta g_{\parallel,\perp} &\approx -3\gamma_0\delta g_{\parallel,\perp};\\
9\pi v^2\partial_t g_\parallel &\approx -8g_\parallel^2 - 20g_\parallel g_\perp + 14g_\perp^2;\\
9\pi v^2\partial_t g_\perp &\approx 4g_\parallel g_\perp - 18g_\perp^2.
\end{aligned} \quad (17)$$

Here $g_\parallel = \gamma_z + 2\gamma_\perp$, $g_\perp = \beta_z + 2\beta_\perp$, $\delta g_\parallel = \gamma_z - \gamma_\perp$, $\delta g_\perp = \beta_z - \beta_\perp$, and t is the logarithm of the running energy.

Solving Eq. (17) down to the energy, $|\varepsilon|$, we find

$$v(\varepsilon) = \left(\frac{\gamma_0}{\pi}\ln\frac{|\varepsilon|}{\varepsilon_0}\right)^{1/2}, \qquad \gamma_0(\varepsilon) = \gamma_0 + \mathcal{O}\left(\frac{g_\parallel(\varepsilon)}{\gamma_0}\right), \quad (18)$$

where $\varepsilon_0 \simeq J\exp(-\pi v_0^2/\gamma_0)$ is the energy at which the first loop RG breaks down, and J is the bandwidth.

The last of Eq. (17) yields nonmixed valleys, $g_\perp = 0$, to be unstable, and $g_\perp$ flows towards

$$g_\parallel(\varepsilon) \approx g_\perp(\varepsilon) \approx 9\gamma_0/\{14\ln[t^*/\ln|\varepsilon|/\varepsilon_0]\}, \quad (19)$$

$\delta g_{\parallel,\perp}(\varepsilon) \propto \ln^3(|\varepsilon|/\varepsilon_0)$, and t^* depends on $g_{\parallel,\perp}(\varepsilon\simeq J)$.

Equation (18) enables one to use the renormalized parameters for the standard calculation of the transport coefficients. The diffusion coefficient $D(\varepsilon)$ is given by

$$D(\varepsilon) = v^2(\varepsilon)\tau_{\rm tr}(\varepsilon)/2, \qquad 1/\tau_{\rm tr}(\varepsilon) = \pi\gamma_0\nu_\varepsilon/4, \quad (20)$$

where $\nu_\varepsilon = |\varepsilon|/[\pi v(\varepsilon)^2]$ is the density of states (per one physical spin). Einstein relation and Eq. (18) yield [17]

$$\sigma = \frac{4e^2}{\pi^2\hbar}\ln\left(\frac{|\varepsilon|}{\varepsilon_0}\right). \quad (21)$$

Equation (21) is the universal formula for the uvLC. It describes either the temperature or the density dependence of the conductivity limited by the short-range disordered potential $|\varepsilon|\to\max(\varepsilon_F, T)$. It also gives the leading dependence of the thermopower through the Mott-Cutler formula. At $|\varepsilon|\lesssim\varepsilon_0$, the logarithms are cut by $1/\tau_{\rm tr}$,

which leads to the replacement of $\ln(\cdots)$ to the factor of the order of unity. The precise value of this factor, however, cannot be calculated within Eq. (17).

$Nl\sigma$ model and localization.—At distances larger than $v/\max(|\varepsilon|, \varepsilon_0)$, soft modes giving rise to uvLC freeze out, and only the degrees of freedom guarded by the fundamental symmetries of the system remain gapless. All those degrees of freedom are described by the $nl\sigma$ model [13] and functional integral (15) is replaced by integral over 16×16 supermatrices in $KK' \otimes AR \otimes eh \otimes g$ space [15]:

$$\langle \ldots \rangle = \int \cdots \exp(-F[\hat{Q}]) \mathcal{D}\hat{Q}, \qquad \hat{Q}^2 = \mathbb{1}, \qquad \hat{Q} = \hat{C}\hat{Q}^T\hat{C}^T, \qquad \hat{Q}^\dagger = \hat{\mathbb{K}}\hat{Q}\hat{\mathbb{K}}, \qquad \hat{\mathbb{K}} = \begin{pmatrix} \mathbb{1}^g & 0 \\ 0 & \tau_3^g \end{pmatrix}_{AR} \otimes \mathbb{1}^{KK'} \otimes \mathbb{1}^{eh}. \quad (22)$$

The free energy functional $F[Q]$ takes the form (the definition of supertrace, Str, can be found in Ref. [13])

$$F = \frac{\pi\nu_\varepsilon}{16} \mathrm{Str} \int \left\{ D(\varepsilon) \left(\nabla\hat{Q} - \frac{ie\mathbf{A}}{c}[\hat{Q}, \hat{\mathcal{T}}_3] \right)^2 + 2i\omega\hat{\Lambda}\hat{Q} - \frac{\pi\nu_\varepsilon g_\parallel}{4}[\hat{\rho}_z, \hat{Q}]^2 - \frac{\pi\nu_\varepsilon g_\perp}{4}([\hat{\rho}_x, \hat{Q}]^2 + [\hat{\rho}_y, \hat{Q}]^2) \right\} d\mathbf{r},$$
$$(\hat{\rho}_\alpha; \hat{\mathcal{T}}_3) = (\tau_\alpha^{KK'} \otimes \mathbb{1}^{eh}; \mathbb{1}^{KK'} \otimes \tau_z^{eh}) \otimes \mathbb{1}^{AR} \otimes \mathbb{1}^g, \quad (23)$$

where $\mathbf{A}$ is the vector potential due to the magnetic field normal to the graphene, and the entries include uvLC.

Equation (23) is the only form allowed by the symmetries of the problem. The symmetries of the Q matrices [Eq. (22)] correspond to the two replicas of symplectic ensemble, which would flow to the limit of large conductances. However, due to $g_{\parallel,\perp} > 0$, only $\hat{Q} \propto \mathbb{1}^{KK'}$ is allowed at large distances, and one obtains a generic orthogonal ensemble. Thus, all the eigenstates are localized. Schematic temperature dependence of σ for undoped graphene is sketched on Fig. 2.

The fist loop correction in Eq. (23) yields the WL [17]:

$$\Delta\sigma_{\mathrm{WL}} = \frac{e^2}{2\pi^2\hbar} \sum_{j=0}^{3} d_j \left[\ln\left(\frac{1}{-i\omega_j\tau_{tr}} \right) - Y\left(\frac{1}{-i\omega_j\tau_B} \right) \right],$$
$$\omega_0 = \omega + i0, \qquad \omega_1 = \omega + \frac{i}{\tau_\perp}, \quad (24)$$
$$\omega_{2,3} = \omega + \frac{i}{2\tau_\parallel} + \frac{i}{2\tau_\perp},$$

where $-d_0 = d_{1,2,3} = 1$, $\tau_{\parallel,\perp}^{-1} = 2\pi\nu_\varepsilon g_{\parallel,\perp}$, $\tau_B^{-1} = 4\mathrm{D}(\varepsilon)eB/(\hbar c)$, $Y(x) = \psi(1/x + 1/2) + \ln x$, and $\psi(x)$ is the digamma function. Inelastic processes are accounted for by $-i\omega \to -i\omega + \tau_\phi^{-1}$, where τ_ϕ is the dephasing time. Equation (24) agrees with Ref. [12]. The new information here is the logarithmic dependence of the parameters on the electron energy; see Eqs. (18)–(20).

In conclusion, we have presented a complete description of a disordered graphene and demonstrated that there are two different types of logarithmic contributions into physical quantities; see Eqs. (21) and (24).

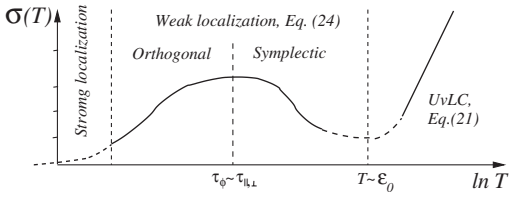

FIG. 2. Schematic dependence, $\sigma(T)$, for the undoped graphene and for $\tau_\phi^{-1} \propto T$. Observation of weak localization (orthogonal case) is reported in the *note added* of Ref. [18].

We are grateful to V. Falko, L. Glazman, and P. Kim for remarks and to Transregio 12 for financial support of K. B. E.

[1] K. S. Novoselov *et al.*, Science **306**, 666 (2004); Nature (London) **438**, 197 (2005); Nature Phys. **2**, 177 (2006).
[2] Y. Zhang *et al.*, Phys. Rev. Lett. **94**, 176803 (2005); Y. Zhang *et al.*, Nature (London) **438**, 201 (2005).
[3] C. Berger *et al.*, J. Phys. Chem. B **108**, 19912 (2004); Science **312**, 1191 (2006); J. S. Bunch *et al.*, Nano Lett. **5**, 287 (2005).
[4] G. L. Bir and G. E. Pikus, *Symmetry and Strain-Induced Effects in Semiconductors* (Wiley, New York, 1974).
[5] J. Tworzydlo *et al.*, Phys. Rev. Lett. **96**, 246802 (2006); V. V. Cheianov and V. I. Falko, Phys. Rev. B **74**, 041403 (2006).
[6] E. Fradkin, Phys. Rev. B **33**, 3257 (1986).
[7] N. H. Shon and T. Ando, J. Phys. Soc. Jpn. **67**, 2421 (1998).
[8] H. Suzuura and T. Ando, Phys. Rev. Lett. **89**, 266603 (2002).
[9] Y. Zheng and T. Ando, Phys. Rev. B **65**, 245420 (2002).
[10] T. Ando, Y. Zheng, and H. Suzuura, J. Phys. Soc. Jpn. **71**, 1318 (2002).
[11] D. V. Khveschenko, Phys. Rev. Lett. **97**, 036802 (2006); A. F. Morpurgo and F. Guinea, *ibid.* **97**, 196804 (2006).
[12] E. McCann *et al.*, Phys. Rev. Lett. **97**, 146805 (2006).
[13] K. B. Efetov, *Supersymmetry in Disorder and Chaos* (Cambridge University Press, New York, 1997).
[14] The matrices $\hat{\Sigma}$, $\hat{z}$ are different from those of Refs. [7,8,12], due to the different choice of the vector in Eq. (1).
[15] I. L. Aleiner and K. B. Efetov (to be published).
[16] This is somewhat similar to that of A. W. W. Ludwig *et al.*, Phys. Rev. B **50**, 7526 (1994).
[17] Here, we restored $\hbar$ and the spin degeneracy.
[18] S. V. Morozov *et al.*, Phys. Rev. Lett. **97**, 016801 (2006).